

A Class of Pb-free Double Perovskite Halide Semiconductors with Intrinsic Ferromagnetism, Large Spin Splitting and High Curie Temperature

Bo Cai,^a Xi Chen,^a Meiqiu Xie,^a Shengli Zhang,^{*,a} Xuhai Liu,^a Jinlong Yang,^b Wenhan Zhou,^a Shiyong Guo,^a Haibo Zeng^{*,a}

^a. MIIT Key Laboratory of Advanced Display Materials and Devices, School of Materials Science and Engineering, Nanjing University of Science and Technology, Nanjing 210094, China. E-mail: zhangslvip@njust.edu.cn, zeng.haibo@njust.edu.cn.

^b. Hefei National Laboratory for Physical Sciences at the Microscale, University of Science and Technology of China, Hefei, Anhui 230026, China.

A. Methods

All the DFT calculations were performed under periodic boundary conditions using the Vienna ab simulation package (VASP).¹ The projector-augmented-wave (PAW) method with a plane-wave basis set was used.^{2, 3} Spin orbit coupling (SOC) effect has been widely applied in band-gap calculations due to the presence of Cs element. However, the SOC effect shows trivial influence on band gaps because that Cs does not participate in electronic transitions in our case. Therefore, it is not adopted in our calculation.⁴ To account for the van der Waals interactions between Cs atoms and other atoms, DFT-D3 method was adopted.⁵ A kinetic energy cutoff of 500 eV was set on a grid of $5 \times 5 \times 5$ k-points for perovskite. Geometry optimization and stability analysis were carried out under the Perdew, Burke, and Ernzerhof (PBE) exchange-correlation functional.⁶ Electronic properties were also extracted by using generalized gradient functional (GGA). To properly describe the strongly correlated electrons in the partially filled d subshells, we used the Hubbard U_{eff} to correct the electronic properties introduced by Dudarev *et al.*⁷ The Hubbard U_{eff} is defined as $U_{\text{eff}}=U-J$, where U and J specifies the on-site Coulomb and exchange interaction parameters, respectively. The self-consistent U_{eff} = 4.13 eV, 2.77 eV, 2.68 eV, 4.73 eV, 6.22 eV, 5.83 eV, 6.52 eV, and 5.38 eV for Ti, V, Cr, Mn, Fe, Co, Ni and Cu, which were extracted from first-principles. Computational method of self-consistent U_{eff} can be found in section D. Self-consistent U_{eff} . Band structures were also checked by Heyd-Scuseria-Ernzerhof hybrid functional (HSE06). The comparison of HSE06 and GGA+ U_{eff} clearly confirm that GGA+ U_{eff} is an accurate method to describe the electronic properties. The parameter reliability was verified by the optimized cubic perovskite CsPbBr_3 lattice parameters of $a = 5.85 \text{ \AA}$ ($a = 5.80 \text{ \AA}$ in Ref. 8).

B. Dynamic stability derived from phonon spectra

The harmonic phonon spectrum was calculated from second-order interatomic force constants obtained by using the real-space finite-difference approach implemented in Phonopy code.⁹ The $2 \times 2 \times 2$ supercell of the primitive cell accompanying with the k-point mesh with grid spacing of $2\pi \times 0.03 \text{ \AA}^{-1}$ was used for these calculations. The room-temperature (300 K) phonon spectrum was obtained by considering an harmonic phonon-phonon interaction with a self-consistent ab initio lattice dynamical (SCAILD) method.¹⁰ This was carried out via calculating the phonon frequencies renormalization induced by phonon entropy, i.e., the geometric disorder introduced by several frozen phonons simultaneously presenting in the simulated supercell. The SCAILD method calculation mainly consists of two cyclic steps. One is to create new atomic displacement in terms of phonon frequencies, and the other is to generate new phonon frequencies from calculated forces acting on the displace atoms. The self-consistent cycle was terminated when the difference in the approximate free energy between two consecutive iterations was less than 1 meV. Calculations were performed at constant volume with ignored thermal expansion effect.

C. Phase stability diagram analysis

In thermodynamic equilibrium growth conditions, the existence of Cs_2GeMX_6 should satisfy

$$2\mu_{\text{Cs}} + \mu_{\text{Ge}} + \mu_{\text{M}} + 6\mu_{\text{X}} = \Delta H(\text{Cs}_2\text{GeMX}_6) \quad (1)$$

where μ_i is the chemical potential of constitute element which refers to its most stable phase, and $\Delta H(\text{Cs}_2\text{GeMX}_6)$ is the formation enthalpy of Cs_2GeMX_6 . To avoid precipitation of the elemental dopants and the host elements, chemical potential μ_i are bound by

$$\mu_i < 0 \quad (2)$$

To avoid the formation of possible secondary phases, the following constraints are required to satisfy simultaneously

$$\begin{aligned}
\mu_{Cs} + \mu_X &< \Delta H(CsX) \\
\mu_{Ge} + a\mu_X &< \Delta H(GeX_a) \\
a\mu_{Ge} + b\mu_M &< \Delta H(Ge_aM_b) \\
\mu_{Ge} + \mu_{Cs} &< \Delta H(CsGe) \\
a\mu_M + b\mu_X &< \Delta H(M_aX_b) \\
a\mu_{Cs} + b\mu_M + c\mu_X &< \Delta H(Cs_aM_bX_c) \\
a\mu_{Cs} + b\mu_{Ge} + c\mu_X &< \Delta H(Cs_aGe_bX_c)
\end{aligned} \tag{3}$$

all the decomposition channels were taken fully into account for various combinations of the competing phases, including all the existing binary, ternary, and quaternary compounds from the Crystallography Open Database.

D. Self-consistent U_{eff}

We calculated Hubbard U_{eff} self-consistently (SCF- U_{eff}) from first-principles by using the linear response approach proposed by Cococcioni and Gironcoli,¹¹ in which U_{eff} is determined by difference between the screened and bare second derivative of the energy with respect to localized state occupations n^I at site I . This can be written as

$$U = \frac{\partial^2 E^{GGA}}{\partial (n^I)^2} - \frac{\partial^2 E_0^{GGA}}{\partial (n^I)^2} \tag{4}$$

Applying localized potential shifts to the d levels transition metal atoms to excite charge fluctuation on their orbitals, and solving the Kohn-Sham equations self-consistently, we can get an occupation dependent energy functional

$$E^{GGA} = \min \{ E[\{\alpha_I\}] - \sum_I \alpha_I n^I \} \tag{5}$$

and

$$\frac{\partial E^{GGA}}{\partial n^I} = -\alpha_I(\{n^I\}), \frac{\partial^2 E^{GGA}}{\partial (n^I)^2} = -\frac{\partial \alpha_I(\{n^I\})}{\partial n^I} \quad (6)$$

Using α_I as the perturbation parameter, the effective interaction parameter U of site I can be obtained as,

$$U = \frac{\partial \alpha_{I,0}}{\partial n_I} - \frac{\partial \alpha_I}{\partial n_I} = [\chi_0^{-1} - \chi^{-1}]^I \quad (7)$$

In the above derivation U_{eff} is calculated from the GGA ground state. It should be consistently obtained from the GGA+ U_{eff} ground state itself, which may be especially relevant when GGA and GGA+ U_{eff} differ qualitatively. To solve this problem (metal versus insulator in the solid state, different symmetry in a molecule), Kulik *et al.* have identified that the electronic terms in the GGA+ U_{eff} functional that have quadratic dependence on the occupations:¹²

$$E_{\text{quad}} = \frac{U_{\text{scf}}}{2} \sum_I [\sum_i n_i^I (\sum_j n_j^I - 1)] + \frac{U_{\text{in}}}{2} \sum_I \sum_i n_i^I (1 - n_i^I) \quad (8)$$

Where SCF- U_{eff} represents the effective on-site electron-electron interaction already present in the GGA energy functional for the GGA+ U_{eff} ground state when U is chosen to be U_{in} . The second derivative of E_{quad} with respect to n_i^I also corresponds to the U_{out} obtained from linear-response:

$$U_{\text{out}} = \frac{d^2 E_{\text{quad}}}{d(\lambda_T^I)^2} = U_{\text{scf}} - \frac{U_{\text{in}}}{m} \quad (9)$$

Thus, U_{out} is linear in U_{in} for the relevant range of $U_{\text{in}}-U_{\text{scf}}$. From a few linear-response calculations for different U_{in} ground states, we can extract the SCF- U_{eff} that should be used for the halide double perovskites. The SCF- U_{eff} is performed using the quantum espresso code⁹ using the GGA (PBE) exchange-correlation functional and PAW pseudopotentials. The wavefunction and electronic density cut-off energies are 35 and 300 Ry, respectively, which are tested to be large enough for the desired accuracy.

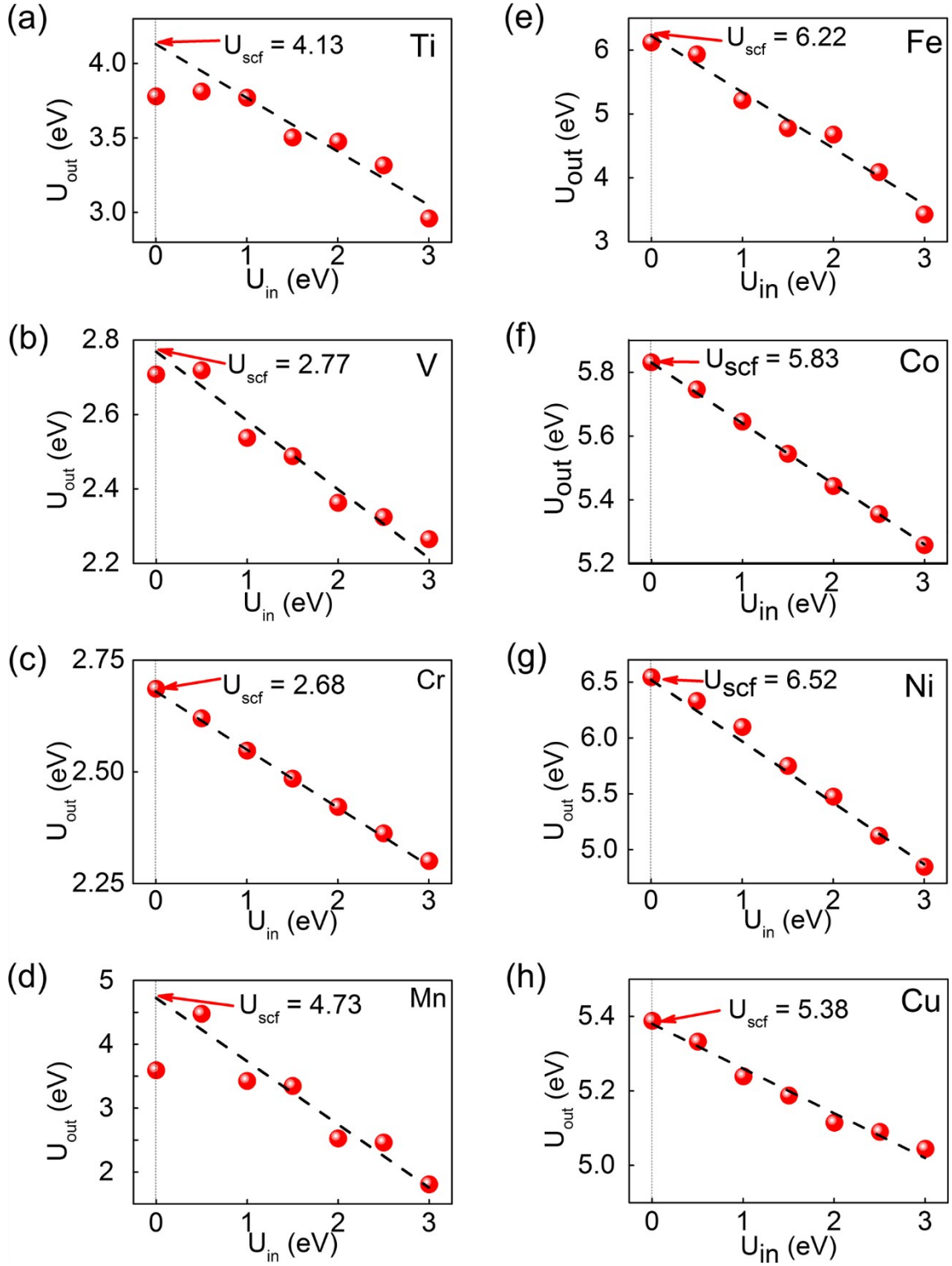


Fig. S1. Linear response U_{out} calculated from the GGA+ U_{in} ground state of $\text{Cs}_2\text{GeMBr}_6$ ($M=\text{Ti}, \text{V}, \text{Cr}, \text{Mn}, \text{Fe}, \text{Co}, \text{Ni}, \text{Cu}$), respectively.

Because the U_{eff} for different compounds strongly affect the electronic properties, and they strongly depend on their bonding environment. We calculate the self-consistent U_{eff} before

checking the electronic properties. Chloride, bromide, and iodide have similar bonding environment, hence we just calculate the self-consistent U_{eff} in $\text{Cs}_2\text{GeMnBr}_6$. Here we plot U_{out} as a linear function of U_{in} , as shown in Fig S1. Hence, the extrapolated self-consistent U_{eff} for Ti, V, Cr, Mn, Fe, Co, Ni, and Cu are 4.13, 2.77, 2.68, 4.73, 6.22, 5.83, 6.52, and 5.38 eV, respectively. The $U = 2.68$ eV of Cr-based halide compounds in our simulation are in excellent agreement with Ref. 13.

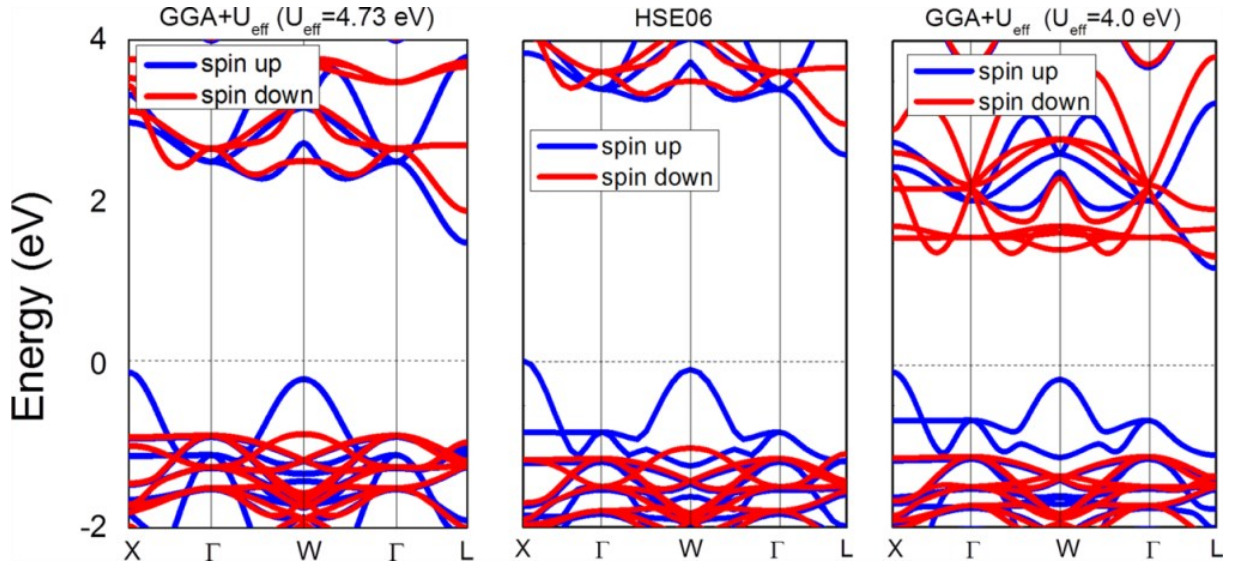


Fig. S2. Comparison of spin-polarized band structures of $\text{Cs}_2\text{GeMnBr}_6$ by using GGA+ U_{eff} ($U_{\text{eff}} = 4.73$ eV), HSE06 and GGA+ U_{eff} ($U_{\text{eff}} = 4.00$ eV) method, respectively.

To further confirm the reasonableness of self-consistent U_{eff} , we compare the spin band structures of $\text{Cs}_2\text{GeMnBr}_6$ by using GGA+ U_{eff} (self-consistent $U_{\text{eff}} = 4.73$ eV and reference value $U_{\text{eff}} = 4.0$ eV in MnO^{14}) and HSE06 methods. HSE06 usually gives an exact description of band structures, but its computational burden is much more expensive than GGA functional. From Fig. S2, we can see that all the features of HSE06 result are reproduction in result of $U_{\text{eff}} = 4.73$ eV, only except bandgap value. Meanwhile, the spin down conduction bands in $U_{\text{eff}} = 4.0$ eV result have obvious difference from HSE06 method and $U_{\text{eff}} = 4.73$ eV. This comparison further reflects the fact that GGA functional combination with self-consistent U_{eff} can give a reasonable description of electronic properties with cheap computational cost.

E. Structures

TABLE 1 Calculated results of cubic lattice constant (a), Ge-X and M-X bond length (l_{Ge-X} , and l_{M-X}), ground state, *etc.* The parameter reliability is confirmed by the optimized cubic perovskite CsPbBr₃ lattice parameters.

	a	bond length		ground states	stable area in phase stability diagram
		l_{Ge-X}	l_{M-X}		
CsPbBr ₃	5.85(cal)	--	--	NM	--
	5.80(exp)	--	--	NM	--
Cs ₂ GeTiCl ₆	10.63	2.69	2.62	AFM	Y
Cs ₂ GeTiBr ₆	11.20	2.82	2.77	AFM	Y
Cs ₂ GeTiI ₆	12.04	3.02	2.98	AFM	Y
Cs ₂ GeVCl ₆	10.49	2.68	2.56	FM	Y
Cs ₂ GeVBr ₆	11.08	2.83	2.70	FM	Y
Cs ₂ GeVI ₆	11.89	3.02	2.93	FM	Y
Cs ₂ GeCrCl ₆	10.39	2.68	2.53	AFM	Y
Cs ₂ GeCrBr ₆	10.96	2.82	2.67	AFM	Y
Cs ₂ GeCrI ₆	11.86	2.99	3.00	AFM	Y
Cs ₂ GeMnCl ₆	10.53	2.69	2.58	FM	Y
Cs ₂ GeMnBr ₆	11.10	2.82	2.73	FM	Y
Cs ₂ GeMnI ₆	11.92	3.01	2.95	FM	Y
Cs ₂ GeFeCl ₆	10.44	2.69	2.55	AFM	N
Cs ₂ GeFeBr ₆	11.03	2.81	2.72	AFM	N
Cs ₂ GeFeI ₆	11.65	3.03	2.79	AFM	N
Cs ₂ GeCoCl ₆	10.19	2.66	2.43	AFM	N
Cs ₂ GeCoBr ₆	10.75	2.79	2.58	AFM	N
Cs ₂ GeCoI ₆	11.73	3.00	2.82	AFM	N
Cs ₂ GeNiCl ₆	10.33	2.69	2.48	FM	N
Cs ₂ GeNiBr ₆	10.90	2.82	2.63	FM	N
Cs ₂ GeNiI ₆	11.67	3.00	2.84	FM	N
Cs ₂ GeCuCl ₆	10.23	2.60	2.52	NM	N
Cs ₂ GeCuBr ₆	10.80	2.73	2.67	NM	N
Cs ₂ GeCuI ₆	11.57	2.91	2.88	NM	N

F. Spin polarized band structure

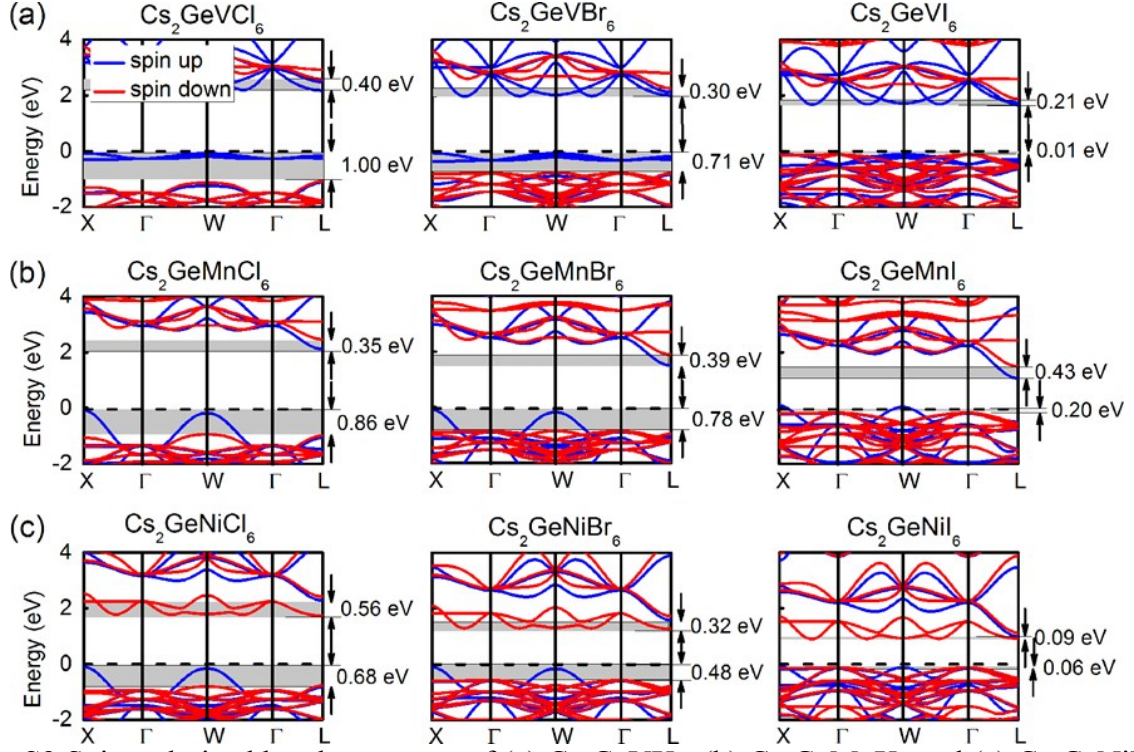


Fig. S3 Spin-polarized band structures of (a) Cs_2GeVX_6 , (b) $\text{Cs}_2\text{GeMnX}_6$ and (c) $\text{Cs}_2\text{GeNiX}_6$. Blue and red lines represent the spin-up and spin-down states, respectively. The width of the gray region represents the spin splitting value.

G. Exchange parameter

TABLE 2 The nearest and next nearest exchange parameter J_1 and J_2 (in meV), energy band

gaps (E_g , in eV), and magnetic moments per magnetic atom (M , in μ_B) for halide double perovskites by using GGA+ U_{eff} method. The energy difference between FM, AFM and NM is also given ($E_{\text{FM}}-E_{\text{AFM1}}$, $E_{\text{FM}}-E_{\text{AFM2}}$, and $E_{\text{FM}}-E_{\text{NM}}$, in meV/atom).

	J_1	J_2	E_g	M	$E_{\text{FM}}-E_{\text{AFM1}}$	$E_{\text{FM}}-E_{\text{AFM2}}$	$E_{\text{FM}}-E_{\text{NM}}$
$\text{Cs}_2\text{GeTiCl}_6$	8.56	3.64	2.32	2	6.85	7.32	--
$\text{Cs}_2\text{GeTiBr}_6$	8.13	3.46	2.11	2	6.50	6.95	-178
$\text{Cs}_2\text{GeTiI}_6$	7.75	3.20	1.87	2	6.20	6.57	--
$\text{Cs}_2\text{GeVCl}_6$	-9.47	-1.37	2.26	3	-17.05	-14.63	--
$\text{Cs}_2\text{GeVBr}_6$	-8.53	-1.24	2.04	3	-15.35	-13.19	-189
Cs_2GeVI_6	-7.40	-1.09	1.78	3	-13.32	-11.46	--
$\text{Cs}_2\text{GeCrCl}_6$	7.15	3.03	0	4	22.88	24.43	--
$\text{Cs}_2\text{GeCrBr}_6$	4.00	1.70	0	4	12.80	13.68	-188
$\text{Cs}_2\text{GeCrI}_6$	2.86	1.19	0	4	9.152	9.72	--
$\text{Cs}_2\text{GeMnCl}_6$	-8.56	-3.75	2.21	5	-42.80	-46.16	--
$\text{Cs}_2\text{GeMnBr}_6$	-7.76	-3.38	1.59	5	-38.80	-41.78	-191
$\text{Cs}_2\text{GeMnI}_6$	-6.82	-2.99	1.05	5	-34.10	-36.79	--
$\text{Cs}_2\text{GeFeCl}_6$	5.98	2.53	2.25	4	19.14	20.42	--
$\text{Cs}_2\text{GeFeBr}_6$	5.91	2.51	1.84	4	18.91	20.21	-141
$\text{Cs}_2\text{GeFeI}_6$	5.76	2.40	1.43	4	18.43	19.58	--
$\text{Cs}_2\text{GeCoCl}_6$	6.26	2.61	1.45	3	11.27	11.97	--
$\text{Cs}_2\text{GeCoBr}_6$	5.54	2.35	1.07	3	9.97	10.65	-135
$\text{Cs}_2\text{GeCoI}_6$	4.80	2.03	0.63	3	8.64	9.22	--
$\text{Cs}_2\text{GeNiCl}_6$	-6.15	-3.24	1.82	2	-4.92	-5.63	--
$\text{Cs}_2\text{GeNiBr}_6$	-5.50	-2.89	1.37	2	-4.40	-5.03	-129
$\text{Cs}_2\text{GeNiI}_6$	-4.80	-2.52	0.97	2	-3.84	-4.39	--
$\text{Cs}_2\text{GeCuCl}_6$	--	--	0	0	--	--	--
$\text{Cs}_2\text{GeCuBr}_6$	--	--	0	0	--	--	--
$\text{Cs}_2\text{GeCuI}_6$	--	--	0	0	--	--	--

We have assigned the initial magnetic moments to $\text{Cs}_2\text{GeMBr}_6$ before the FM and AFM structural optimization. Afterwards, we found that the initial magnetic moment of Cs, Ge, Br and Cu have disappeared. Therefore, we could not extract the energy difference between FM, AFM and NM state $\text{Cs}_2\text{GeCuBr}_6$. Next, we have tried to calculate the system energy of NM state $\text{Cs}_2\text{GeMBr}_6$ (excluding $M=\text{Cu}$). The result demonstrates that the energy of NM $\text{Cs}_2\text{GeMBr}_6$ (excluding $M=\text{Cu}$) is higher than the FM and AFM states. Hence, two conclusions

can be obtained: (i) the magnetism of $\text{Cs}_2\text{GeMBr}_6$ (excluding $\text{M}=\text{Cu}$) is originated from the transition metal atoms. (ii) the ground state of $\text{Cs}_2\text{GeCuBr}_6$ is NM. Based on the two conclusions, we did not simulate the properties of NM Cs_2GeMX_6 ($\text{X}=\text{Cl}$ and I).

References

1. G. Kresse and J. Furthmüller, *Phys. Rev. B*, 1996, **54**, 11169.
2. G. Kresse and D. Joubert, *Phys. Rev. B*, 1999, **59**, 1758-1775.
3. P. E. Blöchl, *Phys. Rev. B*, 1994, **50**, 17953.
4. W.-J. Yin, J.-H. Yang, J. Kang, Y. Yan and S.-H. Wei, *J. Mater. Chem. A*, 2015, **3**, 8926-8942.
5. S. Grimme, J. Antony, S. Ehrlich and H. Krieg, *J. Chem. Phys.*, 2010, **132**, 154104.
6. J. P. Perdew, K. Burke and M. Ernzerhof, *Phys. Rev. Lett.*, 1996, **77**, 3865-3868.
7. S. Dudarev, G. Botton, S. Savrasov, C. Humphreys and A. Sutton, *Phys. Rev. B*, 1998, **57**, 1505.
8. J. Song, J. Li, X. Li, L. Xu, Y. Dong and H. Zeng, *Adv. Mater.*, 2015, **27**, 7162-7167.
9. G. Paolo, B. Stefano, B. Nicola, C. Matteo, C. Roberto, C. Carlo, C. Davide, L. C. Guido, C. Matteo, D. Ismaila, C. Andrea Dal, G. Stefano de, F. Stefano, F. Guido, G. Ralph, G. Uwe, G. Christos, K. Anton, L. Michele, M.-S. Layla, M. Nicola, M. Francesco, M. Riccardo, P. Stefano, P. Alfredo, P. Lorenzo, S. Carlo, S. Sandro, S. Gabriele, P. S. Ari, S. Alexander, U. Paolo and M. W. Renata, *J. Phys-Condens Mat.*, 2009, **21**, 395502.
10. P. Souvatzis, O. Eriksson, M. I. Katsnelson and S. P. Rudin, *Phys. Rev. Lett.*, 2008, **100**, 095901.
11. X. Wu, D. Vanderbilt and D. R. Hamann, *Phys. Rev. B*, 2005, **72**, 035105.

12. H. J. Kulik, M. Cococcioni, D. A. Scherlis and N. Marzari, *Phys. Rev. Lett.*, 2006, **97**, 103001.
13. J. Liu, Q. Sun, Y. Kawazoe and P. Jena, *Phys. Chem. Chem. Phys.*, 2016, **18**, 8777.
14. L. Wang, T. Maxisch and G. Ceder, *Phys. Rev. B*, 2006, **73**, 195107.